Supramolecular Elastomers: Switchable Mechanical Properties and Tuning Photohealing with Changes in Supramolecular Interactions

Anton O. Razgoniaev ⁽¹⁾, ^{1,2} Kirill I. Mikhailov, ^{1,2,3} Filipp A. Obrezkov, ^{1,2,4} Evgeniia V. Butaeva, ⁵ Alexis D. Ostrowski ⁽¹⁾, ²

Correspondence to: A. D. Ostrowski (E-mail: alexiso@bgsu.edu)

Received 4 December 2017; accepted 20 January 2018; published online 00 Month 2018

DOI: 10.1002/pola.28972

ABSTRACT: To study light-triggered self-healing in supramolecular materials, we synthesized supramolecular thermoplastic elastomers with mechanical properties that were reversibly modulated with temperature. By changing the supramolecular architecture, we created polymers with different temperature responses. Detailed characterization of the hydrogen-bonding material revealed dramatically different temperature and mechanical stress response due to two different stable states with changes in the hydrogen bonding interactions. A semicrystalline state showed no response to oscillatory shear deformations while the melt state behaved as a typical energy dissipative material with a clear crossover between storage and loss moduli. Comparison studies on heat generation after light excitation revealed no differences in photo-thermal conversion when an Fe(II)-phenanthroline chromophore was either

physically blended into the H-bonding polymer or covalently attached to the supramolecular network. These materials showed healing of scratches with light-irradiation, as long as the overlap of material absorbance and laser excitation was sufficient. Differences in the efficiency and rate of photohealing were observed, depending on the type of supramolecular interaction, and these were attributed to the differences in the thermal response of the materials' moduli. Such results provide insight into how materials can be designed with chromophores and supramolecular bonding interactions to tune the lighthealing efficiency of the materials. © 2018 Wiley Periodicals, Inc. J. Polym. Sci., Part A: Polym. Chem. 2018, 00, 000–000

KEYWORDS: hydrogen-bonding; light-to-heat conversion; photoresponsive materials; self-healing; supramolecular polymers

INTRODUCTION To create next-generation materials it is necessary to design-specific bonding interactions into the material to control the material properties. Stimuli-responsive materials are promising, since this allows for precise control of the bonding interactions in the polymer using external stimuli. One possible design of such materials is a low molecular weight amorphous polymer backbone with dynamic bonds such as hydrogen (H-bonding) or metal coordination bonds. These interactions link short polymer molecules together to create a supramolecular network that provides toughness and elasticity to the bulk material, but allow for a dynamic response to the external stimulus.

In the past decade, there have been several reports on supramolecular thermoplastics – materials with both an amorphous polymer backbone chain and a well-ordered supramolecular network – that create crystalline segments or clusters in the

material. One approach to create these ordered crystalline domains in the supramolecular thermoplastics is based on the modification of end-groups of low molecular weight telechelic polymers with multiple hydrogen bonding dynamic motifs that "stick" together and assemble into a supramolecular network in the solid state.²²⁻³¹ Another technique to design a more sophisticated supramolecular architecture in the polymer matrix utilizes dynamic-bonding interactions between the polymer end-group^{32,33} or side chain of block copolymers^{34–38} and small molecules. It is a challenge to make these materials have stimuli-responsive properties, however, since the key design feature of this class of supramolecular materials is based on complex interactions of multiple hydrogen-bonding motifs, which suffer from non-ideal photochemical properties such as a lack of visible light absorption. This limits them as stimulus-responsive materials, significantly reducing the capacity to respond to light stimuli. 4,8,39-47 Alternatively, in

Additional Supporting Information may be found in the online version of this article.

© 2018 Wiley Periodicals, Inc.



¹Department of Chemistry, Bowling Green State University, 141 Overman Hall, Bowling Green, Ohio 43403

²Center for Photochemical Sciences, Bowling Green State University, 141 Overman Hall, Bowling Green, Ohio 43403

³Institute of Chemistry, Saint-Petersburg State University, Universitetskii pr. 26, 198504, St, Petersburg, Russia

⁴Skolkovo Institute of Science and Technology, Skolkovo Innovation Center, Nobel St. 3, Moscow 143026, Russia

⁵KLA-Tencor, 1 Technology Dr, Milpitas, California 95035

supramolecular materials using metal coordination motifs, the metal coordination center can also serve as chromophore 48 so that visible light irradiation can be used to control the metalligand interactions. 47

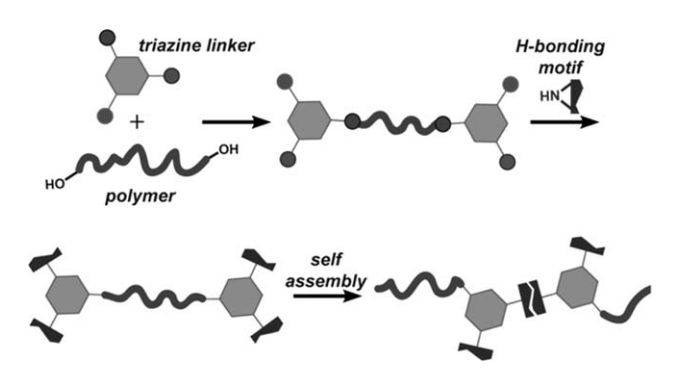
Light-responsive materials that utilize a variety of different metal-coordination bonding interactions - classic metalcoordination interactions and metal nanoparticles - have been designed. 40,49-52 In these materials, healing was observed due to local heat generation from the light irradiation - usually because of the high absorbance of the UV light used - which led to breaking of the supramolecular interactions in the local irradiation volume. 40,49 In contrast, our group has recently shown that materials can be designed with light-induced bond labilization, where visible light irradiation can be used to reversibly soften materials, beyond that of any light to heat generation.⁴⁷ These results evoke a question: is it necessary, or better, to include the chromophore as part of the supramolecular structure and break the metal coordination bonds, or is it sufficient to just generate heat from chromophore being dispersed into the polymer matrix? Understanding the photophysics and photochemistry of the chromophores in these supramolecular materials is critical then, to elucidate how light irradiation can be used to control the bonding interactions in the polymers, and ultimately the mechanical properties of materials.

To fully characterize how a light stimulus to a chromophore can be used to control mechanical properties in supramolecular materials, we prepared new supramolecular polymers with both H-bonding (Scheme 1) and metal coordination bonding motifs, and compared the heat generation and self-healing of these materials upon light irradiation. Specifically we created a hydrogen-bonding supramolecular polymer with multiple molecular recognition elements with thermoplastic mechanical properties that can be reversibly modulated through changing the hierarchy of the supramolecular architecture from crystalline to disordered. These two disordered and crystalline materials had the same chemical composition of the building units, and can act as a supramolecular thermoplastic or as a viscoelastic polymer melt based on assembly of the H-bonding network. We measured the heat generation and self-healing of polymers with different bonding interactions using Fe(II)-phenanthroline as a chromophore. We used IR thermography to determine the heat generated in the materials during light irradiation, and showed that regardless of whether the absorber is a part of the supramolecular assembly or dispersed in the Hbonding polymer, it generates about the same amount of heat.

EXPERIMENTAL

Materials

Krasol HLBH-P 3000 polymer (hydroxyl terminated hydrogenated poly(ethylene-co-butylene)) was purchased from Cray Valley SA. Diisopropylethylamine (DIPEA, 98%), ethanolamine (99%), *N*-methylethanolamine (98%), phenylisocyanate (98%), oxalyl chloride (99%) were purchased from Sigma-Aldrich and stored under inert atmosphere. Celite 545, Na₂SO₄ (anhydrous), CDCl₃ (99.5%), 1,10-phenanthrolin-5-amine



SCHEME 1 General synthetic scheme to create supramolecular polymers using *sym*-trichlorotriazine chemistry.

from Sigma-Aldrich were used as received. *tris*-(3,4,7,8-tetramethyl-1,10-phenanthroline)iron(II) sulfate was received from ICN pharmaceuticals. *sym-*Trichlorotriazine was purchased from TCI and stored under inert atmosphere in the freezer. All solvents (EMD) were dried over 4 Å molecular sieves.

Synthesis of Polymers

Detailed synthetic procedures with schemes (Schemes S1–S7) and NMR characterization (Figures S1–S6) are available in the Supporting Information.

Briefly, the introduction of H-bonding motifs was accomplished in two steps upon heating of polymer (1) (Scheme S1) in excess of 2-ethanolamine to obtain polymer (2) (Supporting Information Scheme S2). Further reaction of the free hydroxyl-groups of polymer (2) with phenyl isocyanate yielded a supramolecular H-bonded polymer P1 (Supporting Information Scheme S4). The H-bonded polymer P2 was synthesized in the similar fashion as P1: Triazine-terminated HLBH-P 3000 (1) was sequentially reacted with N-methylethanolamine and phenyl isocyanate to obtain polymer (3) and supramolecular polymer P2 (Supporting Information Schemes S3 and S5). Metallosupramolecular polymer P3, (Supporting Information Scheme S7), was obtained from first synthesis of a precursor oxalyl monochloride terminated HLBH-P 3000 polymer (4) by reaction of HLBH-P 3000 and excess of oxalyl chloride (Scheme S6). Polymer P3 was then synthesized by reaction of polymer (4) and 5-amino-1,10phenanthroline, with subsequent addition of 25% stoichiometric required amounts of Fe(OTf)₂ in methanol/chloroform solvent mixture. The ratio of Fe(II) ions to phenanthroline terminated HLBH-P (5) was chosen to decrease the optical density of the material and make the polymer film thick enough for self-healing studies.

General Characterization

NMR was recorded on a Bruker AVANCE III spectrometer operating at 500 MHz. Steady-state UV-vis absorption spectra were recorded with a Shimadzu UV-2600 spectrophotometer with 0.5 nm resolution. Differential scanning calorimetry traces were obtained using DSC Q2000 system at a heating rate of 10 °C min $^{-1}$ from -85 °C to 155 °C using sample of approximately 2 mg. Powder X-ray diffraction patterns were recorded

on a Bruker D8 Advance Davinci powder X-ray diffractometer with Cu $K_{\rm x1}$ radiation ($\lambda=1.5406$ Å) within 2θ range from 6 to 40 degrees. FTIR measurements were recorded using a JASCO FTIR-4000 spectrometer on the neat polymer films. The temperature of the irradiation spot of the polymers was determined using a Flir C2 Compact Thermal Imaging System. To account for inhomogeneity of the chromophore distribution along the polymer films, the temperature was determined at three different spots on the material, and recorded temperatures are averages. The microscope images were taken on an OMAX optical microscope equipped with A35140U3 digital camera operating in $\times 4$ magnification mode.

Rheological Characterization

The mechanical properties characterization was performed on a TA Instruments HR2-Discovery hybrid rheometer equipped with a peltier plate in the parallel plates geometry. Due to the presence of multiple H-bonding interactions and the 2 states observed in the H-bonding polymer P1, sample preparation was of great importance for good data reproducibility. First, H-bonded polymer P1 was heated at 110 °C in the oven for 30 min into a Teflon mold to erase the presence of any crystalline domains. Rapid cooling of the polymer with liquid nitrogen provided polymer P1 in the melt state (P1-M). The polymer was placed between the plates of the rheometer and sheared at 0.5 Hz oscillation frequency for 30 min at 5 °C for better adhesion. To recover the crystalline state (P1-X), the viscoelastic polymer mass P1-M was heated at 60 °C for 12 h between the plates of the rheometer.

Time–temperature superposition (TTS) curves were generated based on a set of frequency sweep tests performed on each sample. The frequency sweep experiments were carried out at 0.5% strain and 0.1–10 rad/s frequency range within a 5–50 °C temperature range with 15 °C increments. The reference temperature was 20 °C for all TTS master curves. The TTS tests were performed three times to ensure reproducibility.

Relaxation tests were performed by applying a 0.5% step strain γ , and then the stress σ and relaxation modulus $G(t) = \sigma/\gamma$ were monitored over time at 15 °C.

Density Functional Theory (DFT) Calculations

First, molecular mechanics calculations were performed to permit rapid and extensive conformational searching on hydrogenbonding dimers. After locating the conformational minima, the geometries of the assemblies were calculated by the Density Functional Theory (DFT) using the hybrid of Becke's non-local three parameter exchange and correlation functional with the Lee-Yang-Parr functional (B3LYP)⁵³⁻⁵⁵ using Spartan 16 (Wavefunction, Inc.) software utilizing 6-31* basis set.

Polymer Films Preparation for Self-Healing Tests

A scoop (\sim 2 mg) *tris*-(3,4,7,8-tetramethyl-1,10-phenanthroline)iron(II) sulfate was dissolved in methanol (MeOH). The amount of solvent was adjusted such that 75 μ L of the prepared stock solution diluted in 3 mL of methanol has absorbance equal to 0.5 at the maximum absorbance peak in the UV-vis spectrum. For the self-healing tests, amounts of the

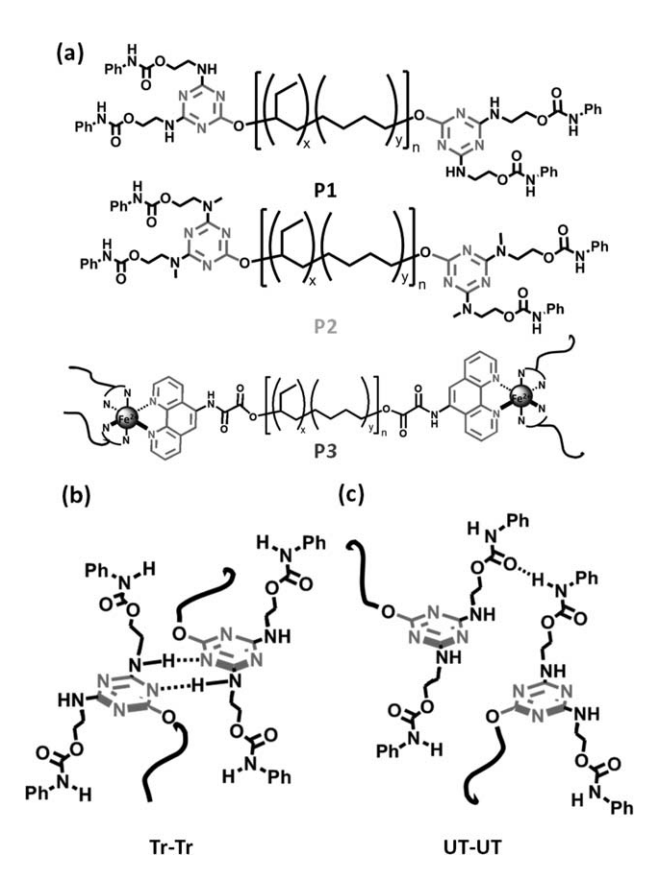


FIGURE 1 (a) Chemical structures of H-bonded supramolecular polymers P1, P2, and metallosupramolecular polymer P3. (b) Triazine–triazine (Tr–Tr) and (c) urethane–urethane (UT–UT) hydrogen-bonding interactions.

chromophore stock solution corresponding to Abs = 0.5 were taken, concentrated to ${\sim}20~\mu L$ and diluted with extra 200 μL of CHCl $_3$. This polymer stock solution 330 μL (40 mg) was added to the chromophore MeOH/CHCl $_3$ solution and well mixed. Then this final polymer/chromophore solution was placed on a microscope slide and the solvent was evaporated to form a solid film. The procedure was repeated until the absorbance of the solid film matched the required value. Prior to self-healing tests, the polymer films were dried in air overnight. The polymer films were cut with a razor blade and the cut area was irradiated with 455 nm CW laser equipped with a 455 nm notch filter and collimating lens at 100–350 mW radiation power with 50 mW increment. The diameter of the laser beam was 2.2 mm. Radiation time was 30 s.

RESULTS AND DISCUSSION

Synthesis of Supramolecular Polymers

We used our previously reported modular synthetic approach to modify polymer termini groups via nucleophilic aromatic substitution of the *sym*-trichlorotriazine ring⁴⁷ to create a series of hydrogenated poly(ethylene-*co*-butylene) polymers (HLBH-P 3000). These polymers all had dynamic bonding motifs that enhanced the elastic properties of the materials via supramolecular interactions [Fig. 1(a)]. Polymer P1 was designed with three H-bonding associates – one



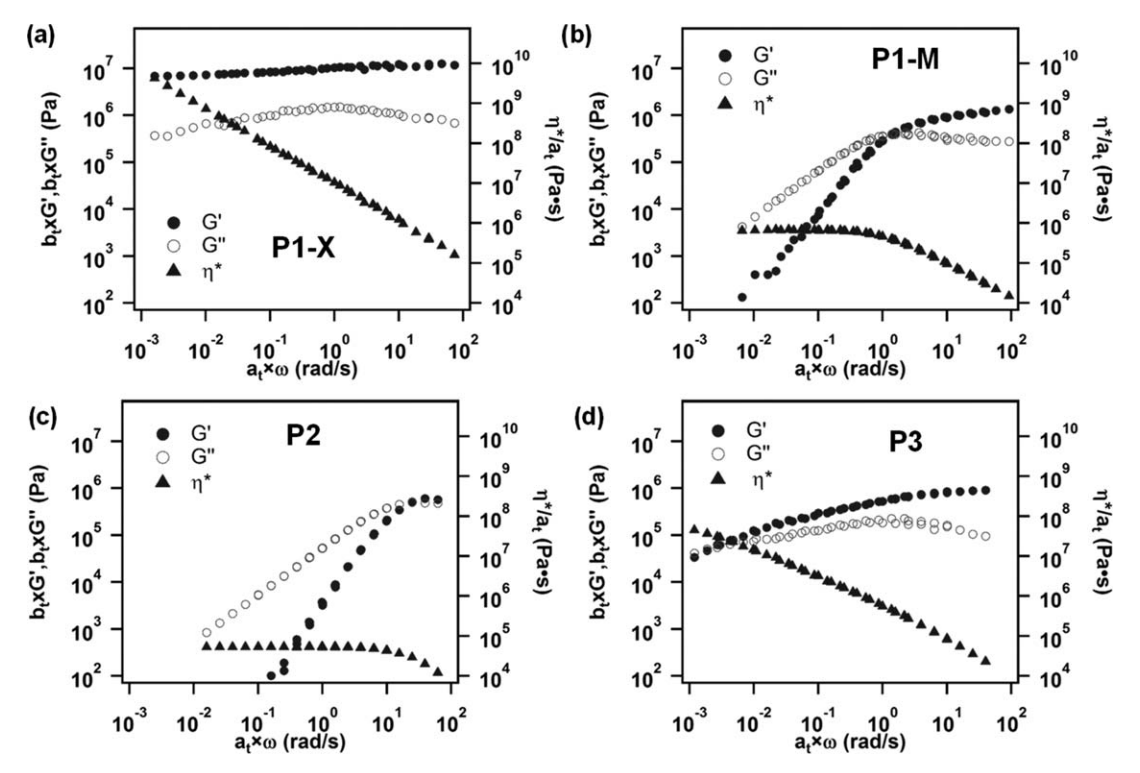


FIGURE 2 (a) Time–temperature superposition (TTS) curves ($T_{ref} = 20$ °C) of (a) crystalline state of polymer P1-X, (b) melt state of polymer P1-M, (c) P2, and (d) metallopolymer P3. Storage modulus is shown as full circles, loss modulus as empty circles, and complex viscosity as triangles.

triazine-triazine (Tr-Tr) and two urethane-urethane (UT-UT) binding groups per polymer termini [Fig. 1(b,c) and Supporting Information Figure S12]. Polymer P2 was synthesized with only two UT-UT per termini, respectively. With the goal of specifically comparing how light irradiation affects the properties of materials with either hydrogen bonding or metal-coordination bonding interactions, a polymer with metal-coordination binding (Polymer P3) was prepared using the Fe(II)-phenanthroline metal-coordination bonding. The starting HLBH-P 3000 was a viscous liquid whereas, in contrast, supramolecular polymer P1 was a solid material (after solution or thermal annealing) and P2 was a viscoelastic melt. Metallopolymer P3 was a viscoelastic material with dark orange/reddish color due to the absorbance of the Fe(II)-phenanthroline moiety with an expected absorbance peak at 515 nm (Supporting Information Fig. S7).

Mechanical Properties of Supramolecular Polymers

The mechanical properties of the supramolecular polymers P1, P2, and P3 were studied by oscillatory rheology. The time-temperature superposition (TTS) master curve for a reference temperature of 20 °C of the solution cast polymer P1 [Fig. 2(a)] revealed that elastic properties dominated over viscous losses (storage modulus G' > loss modulus G'' > loss modulus G' > loss modulus G'

exceeded storage modulus G'. The fact that the polymer P1 with the same chemical composition had temperature controlled response to oscillatory shear stress was indicative of an essentially different hierarchy of the supramolecular architecture. We assigned these architectures as crystalline (P1-X) and melt (P1-M) states of polymer P1 [Fig. 2(a,b)]. To better understand the influence of the multiple hydrogenbonding interactions on the formation of these two different states in polymer P1, the additional H-bonded supramolecular polymer P2 with the same UT-UT but without possibility to form Tr-Tr H-bonding interactions [Fig. 1(a,c)] was prepared for comparison. The TTS master curve of P2 [Fig. 2(c)] displayed oscillatory shear response similar to P1-M rather than P1-X. Thus, both P1-M and P2 revealed TTS curves consistent with viscoelastic polymer melts with a clear crossover between G' and G'' in accordance with their transient hydrogen-bonding cross-links, whereas the P1-X state behaved as a permanently cross-linked covalent network despite being supramolecular polymer.

The metallopolymer P3 with Fe(II)-phenanthroline metal-coordination bonding revealed typical oscillatory shear response (TTS master curve) for energy dissipative materials⁵ [Fig. 2(d)] with a crossover point at $(3 \pm 1) \times 10^{-3}$ rad s⁻¹.

Detailed Characterization of Supramolecular Thermoplastic P1

For a better understanding of how differences in the assembly of hydrogen bonding motifs in the supramolecular

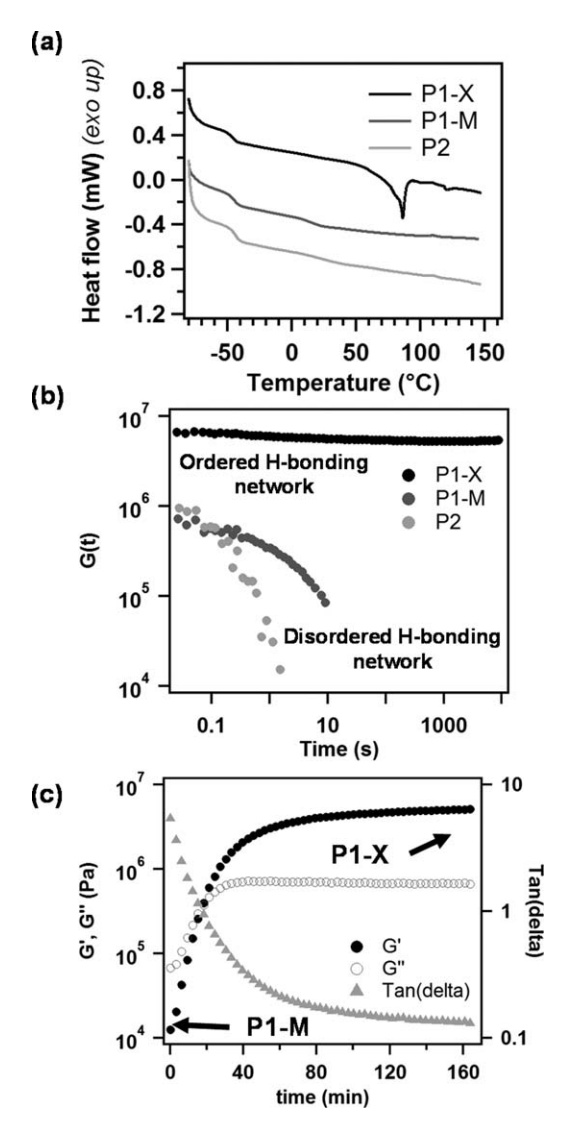


FIGURE 3 (a) Differential scanning calorimetry traces and (b) step strain relaxation curves at 15 °C of P1-X (black), P1-M (dark gray), and P2 (light gray) polymers. (c) $Tan(\delta)$ (gray triangles), storage G' (solid circles), and loss G'' (empty circles) moduli recovery curves from P1-M to P1-X state over time upon heating at 60 °C. The "P1-M" and "P1-X" labels along with the arrows indicate to mechanical properties of corresponding state of the P1 polymer at 60 °C and 1 Hz oscillation frequency.

polymers govern the mechanical properties, we carried out FTIR measurements on the polymer films to determine the type of H-bonding interactions. The FTIR spectrum of the polymer P2 with only UT-UT interactions possible revealed broad signals centered at 3332 cm⁻¹ and 1709 cm⁻¹ assigned to H-bonded N-H stretching and H-bonded C=0 stretching modes of the urethane fragment, respectively (Supporting Information Fig. S8). The infrared spectrum of P1-X showed a much sharper N-H stretching mode at 3332 cm⁻¹ compared to the one in P2 spectrum and a sharp C=0 stretching signal centered at 1700 cm⁻¹. This $\sim 10 \text{ cm}^{-1}$ energy difference between the C=0 stretching of

P1-X and P2 is indicative of the formation of regular wellordered hydrogen bonding network in the P1-X state.⁵⁶⁻⁵⁸ Two new signals centered at 3435 cm⁻¹ and 3258 cm⁻¹ in the P1-X state correspond to vibration of free and hydrogen bonded N—H of the *sym*-triazine, respectively. ⁵⁹⁻⁶¹ Analysis of the infrared absorption profile of the P1-M state showed non-ordered urethane and sym-triazine hydrogen bonding motifs as well as a significant contribution of free urethane fragments (1738 cm⁻¹ C=0 vibration).

To support FTIR and rheology data that suggested the presence of a well-ordered hydrogen bonding network in the P1-X polymer, we performed differential scanning calorimetry (DSC) and powder X-ray diffraction (PXRD) measurements. The DSC trace of the solution cast polymer P1 [Fig. 3(a)] showed an endothermic peak centered at 85 °C, which was assigned to a phase transition between the well-ordered crystalline hydrogen-bonding network (P1-X) and the melt state (P1-M). The second heating cycle of the P1 polymer as well as P2 polymer, however, did not reveal such a characteristic signal at the DSC curve which correlates with viscoelastic nature of both P1-M and P2 polymer and solid-like behavior of the P1-X polymer. It should be noted that both P1 and P2 H-bonding polymers displayed a glass transition temperature at -49 °C on the DSC traces, which corresponds to the soft phase formed by the poly(ethylene-co-butylene) segments. Powder X-ray diffraction (PXRD) measurements also supported the presence of the crystalline domains in the P1-X state (Supporting Information Fig. S9). Heating of the P1-X polymer at 110 °C and rapid cooling with liquid nitrogen, however, erased these small features on the PXRD pattern centered at $2\Theta = 19.2^{\circ}$ and $2\Theta = 21.5^{\circ}$ and left only amorphous halo.

To further investigate the influence of the supramolecular network architecture on the mechanical properties of the materials, step-stress relaxation experiments were performed. After stress was applied, both P1-M and P2 polymer melts relaxed over time since their reversible hydrogen bonding cross-links can be separated followed by diffusion in the polymer matrix, and finally locating a new associative partner [Fig. 3(b)]. In comparison, P1-X with a different hierarchy of the supramolecular architecture (ordered hydrogen bonding network in P1-X versus disorder in P1-M and P2) inhibits the binding motifs to diffuse away and forces them to reconnect back with the old associative partner, which prevents formation of a new supramolecular network. Because the hydrogen-bonding pairs break and re-form many times without the possibility to be separated in the P1-X polymer, the strain energy cannot dissipate, and the observed relaxation time was extremely long [Fig. 3(b)]. Remarkably, such a long relaxation time is more characteristic for permanent covalent networks rather than for supramolecular polymer assemblies.

The transition between the semi-crystalline P1-X and melt P1-M states was reversible and could be achieved in both directions. As previously described, melting and rapid



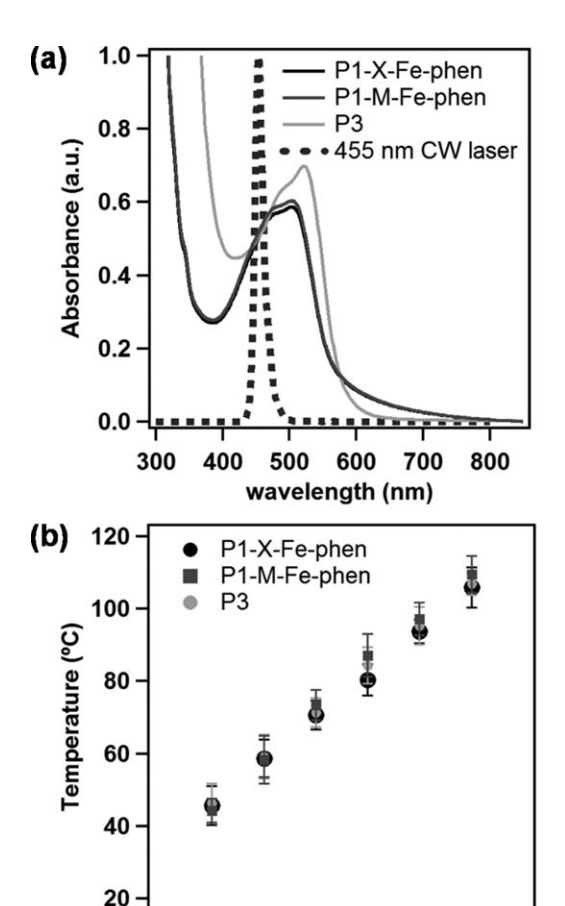


FIGURE 4 (a) Absorbance of the P1-Fe-phen and P3 films. (b) Temperature generated at the 455 nm CW laser radiation as a function of excitation power.

200

Excitation power (mW)

300

400

100

cooling of the P1-X polymer resulted in the viscoelastic material P1-M. The P1-X state, however, could be recovered back upon heating of the melt state at 60 °C for 3-4 h [Fig. 3(c)]. At this temperature, the spontaneously formed hydrogen bonding network undergoes continuous rearrangement, allowing the urethane and triazine binding motifs to find their self-complementary associative partners and reform a well-organized supramolecular network. In other words, the P1-X can be assigned as a thermodynamic "state" and P1-M as a kinetic "state."

Photohealing with Fe(II)-Phenanthroline-Based Chromophore

We compared the differences in photo-thermal effect between physically blended Fe-phen chromophore into the hydrogen-bonded polymer P1 (P1-Fe-phen) versus the metallopolymer P3, where the Fe-phenanthroline moiety was covalently attached to the supramolecular system (Supporting Information Fig. S10). The samples were damaged with well-defined, intersecting cuts with a razor blade, and then irradiated with 455 nm continuous wave (CW) laser radiation (OEM laser system with 455 nm band pass notch filter)

for 30 s at different laser powers. The output powers and corresponding laser flux densities are listed in Supporting Information Table S1. The heat generated in the polymers was determined using an IR camera, and, the temperature of the material increased at the irradiation spot. For more accurate estimates of the relative amount of photons absorbed by each polymer films, we used a modified formula for spectral overlap (S.O.) which estimates the area overlap between the chromophore absorbance and laser excitation profiles (eq 1).

$$J(\lambda) = \int_{0}^{\infty} A_{\rm p}(\lambda) \lambda^{4} F_{\rm laser}(\lambda) d\lambda \tag{1}$$

where $J(\lambda)$ is a spectral overlap, A_p is absorbance of the polymer film, λ is wavelength, F_{laser} is the laser output spectrum normalized to an area of 1. Despite some differences in the absorption profiles of P1-Fe-phen and P3 [Fig. 4(a)], the spectral overlap with the CW laser excitation profile was similar for both polymer films (Supporting Information Table S2). As seen from Figure 4(b), both P1-Fe-phen and P3 films showed a linear increase in temperature generated with increase in laser radiation power. Moreover, regardless of the chromophore being the part of the supramolecular system or not, both polymers P1-Fe-phen and P3 generated about the same amount of heat at each laser excitation power [Fig. 4(b)]. This shows that the chromophore does not have to be chemically incorporated into the material; simply physical blending would give the same photo-thermal effect.

We used optical healing as a visualization tool to observe when the stimulus (light) caused changes in the material. Despite no differences in the heat generated between the two Fe-phen systems (either physically blended chromophore or covalently attached to the supramolecular network), some differences in the healing were observed [Fig. 5(a-c)]. Specifically, the photo-thermal heating of the P1-X-Fe-phen polymer molten the material when a temperature threshold of \sim 70 to 75 °C was reached [Fig. 5(a,d], which correlated with the DSC curve of P1-X [Fig. 3(a)]. The melting of the P1-X polymer occurred only at the radiation area creating a "well" with some invagination involved [see Fig. 5(a)], which shows how precise spatial control of the material melting could be achieved when using light as an external stimulus. Almost immediate disappearance of the damaged area was observed in the P1-M-Fe-phen melt state, which showed some flow characteristics $(\tan(\delta) > 1)$ already at 40 °C [Fig. 5(b,e)]. Metallopolymer P3 slowly flowed upon photoheating of the scratched area in accordance to its viscoelastic behavior, where a gradual disappearance in the scratched area was observed. The temperature threshold to observe some flow in P3, however, was much greater than for P1-M H-bonding polymer, and the healing was observed at much higher laser irradiation power [Fig. 4(b) and 5]. It should be noted that no photohealing was observed in the polymers P1 and P2 without the chromophore (Supporting Information Fig. S11). These results show that the

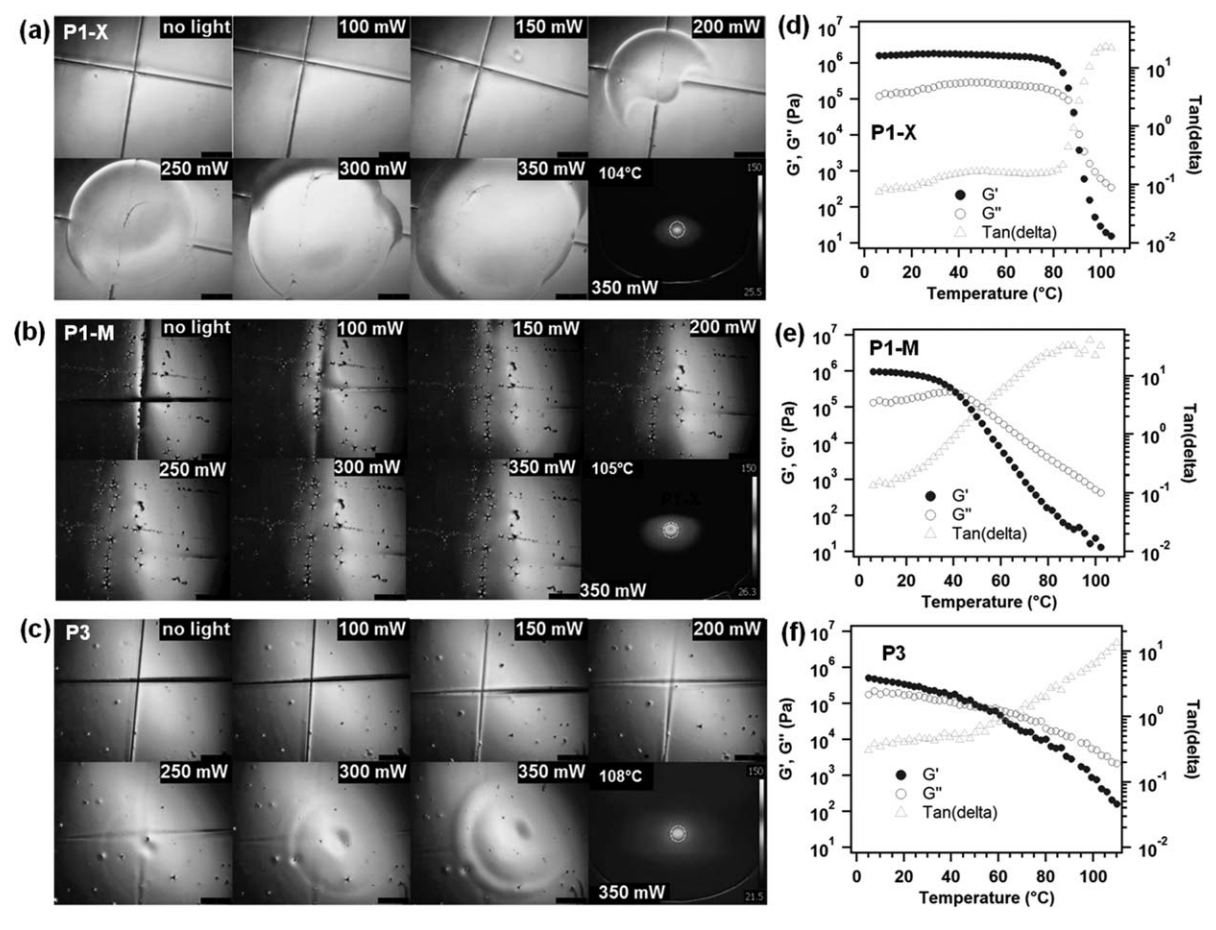


FIGURE 5 Optical images of (a) P1-X-Fe-phen, (b) P1-M-Fe-phen, and (d) P3 mechanically damaged films irradiated at various excitation powers. The black scale bar is 400 μm. The last image in the series shown as an example of IR-camera image taken at the highest radiation power. Temperature sweep curves at 0.5 Hz oscillation frequency of (c) P1-X, d) P1-M, and (e) P3 supramolecular polymers. Storage modulus is shown as full circles, loss modulus as empty circles, and tan(delta) as triangles.

temperature response of the polymer is more important to consider in designing photo-healable materials, and covalent attachment of the chromophore into the network is not necessary to achieve a response.

CONCLUSIONS

Using a modular synthetic method, we were able to create H-bonded and metal coordination supramolecular materials with unique mechanical properties. Particular interesting was the polymer whose mechanical properties could be modified though temperature control of the supramolecular assembly. The amorphous state, where urethane and triazine hydrogen bonding units are randomly bound together or even have no associative partner at all, revealed characteristic oscillatory shear stress response to that of an energy dissipative material. With simple temperature annealing, however, a semicrystalline state could be formed, where most of the hydrogen bonding motifs are bound to their corresponding self-complementary associative partner to form well-ordered supramolecular network. This polymer was used as a platform for detailed investigation of photohealing effect.

Comparison of the photo-self-healing and photo-thermo effects of these supramolecular materials provided some answers to our initial question: Is it necessary to include the chromophore as part of the supramolecular structure to create lightresponsive materials? The answer: Not really. Using the IR imaging, we detected about the same amount of heat generated in polymers with physically dispersed and covalently attached Fe-phen-based chromophore. A more continuous healing was observed for the metallosupramolecular P3 materials compared to the chromophore/P1-X polymer. However, when the polymer P1 melt state was used, a similar slower partial depolymerization of the supramolecular network took place upon thermal breaking H-bonding. As opposed to the viscoelastic materials, in the supramolecular thermoplastic P1-X, the H-bonding network resisted moderate heating until melting region of \sim 70 to 75 $^{\circ}$ C was reached causing the whole H-bonded network to collapse, and polymer filled the damaged area. These results also highlight how metal coordination bonding can be advantageous when creating photohealing materials since it can serve as the chromophore and supramolecular binding motif. This creates a material with gradual photohealing at a relatively high temperature, which avoids any well formation while ensuring the material is stable at higher temperatures.



ACKNOWLEDGMENTS

AOR acknowledges the Center for Photochemical Sciences McMaster Fellowship for partial support. KIM and FAO acknowledge the Center for Photochemical Sciences for summer support. We thank Anne McNeil and Kendra Souther (University of Michigan) for help with DSC measurements. We also thank Jeremy Klosterman for help with PXRD measurements. We thank Niels Holten-Andersen (MIT) for helpful discussions. We acknowledge Andy Torelli and the NSF grant (DUE-1626302) for use of the IR camera. This work was partially supported by an NSF CAREER award, Division of Chemistry, Chemical Structure, Dynamics and Mechanisms- B Program and Division of Materials Research Polymers program (CHE-1653892).

REFERENCES AND NOTES

- 1 G. R. Whittell, I. Manners, Adv. Mater. 2007, 19, 3439.
- **2** C.-A. Fustin, P. Guillet, U. S. Schubert, J.-F. Gohy, *Adv. Mater.* **2007**, *19*, 1665.
- **3** G. R. Whittell, M. D. Hager, U. S. Schubert, I. Manners, *Nat. Mater.* **2011**, *10*, 176.
- **4** J. R. Kumpfer, S. J. Rowan, *J. Am. Chem. Soc.* **2011**, *133*, 12866.
- **5** J. R. Kumpfer, J. J. Wie, J. P. Swanson, F. L. Beyer, M. E. Mackay, S. Rowan, *J. Macromol.* **2012**, *45*, 473.
- **6** X. Yan, F. Wang, B. Zheng, F. Huang, *Chem. Soc. Rev.* **2012**, *41*, 6042.
- **7** D. Mozhdehi, S. Ayala, O. R. Cromwell, Z. Guan, *J. Am. Chem. Soc.* **2014**, *136*, 16128.
- 8 C. Heinzmann, S. Coulibaly, A. Roulin, G. L. Fiore, C. Weder, ACS Appl. Mater. Interfaces 2014, 6, 4713.
- 9 K. Kawamoto, S. C. Grindy, J. Liu, N. Holten-Andersen, J. A. Johnson, ACS Macro Lett. 2015, 4, 458.
- 10 S. C. Grindy, R. Learsch, D. Mozhdehi, J. Cheng, D. G. Barrett, Z. Guan, P. B. Messersmith, N. Holten-Andersen, *Nat. Mater.* 2015, *14*, 1210.
- **11** O. R. Cromwell, J. Chung, Z. Guan, *J. Am. Chem. Soc.* **2015**, 137, 6492
- 12 Y.-L. Rao, A. Chortos, R. Pfattner, F. Lissel, Y.-C. Chiu, V. Feig, J. Xu, T. Kurosawa, X. Gu, C. Wang, M. He, J. W. Chung, Z. Bao, *J. Am. Chem. Soc.* 2016, *138*, 6020.
- 13 D. Mozhdehi, J. A. Neal, S. C. Grindy, Y. Cordeau, S. Ayala, N. Holten-Andersen, Z. Guan, *Macromolecules* 2016, *49*, 6310.
- **14** J.-C. Lai, J.-F. Mei, X.-Y. Jia, C.-H. Li, X.-Z. You, Z. Bao, *Adv. Mater.* **2016**, *28*, 8277.
- 15 J. Cortese, C. Soulié-Ziakovic, S. Tencé-Girault, L. Leibler, J. Am. Chem. Soc. 2012, 134, 3671.
- **16** A. Das, A. Sallat, F. Böhme, M. Suckow, D. Basu, S. Wiessner, K. W. Stöckelhuber, B. Voit, G. Heinrich, *ACS Appl. Mater. Interfaces* **2015**, *7*, 20623.
- 17 C. Xu, L. Cao, B. Lin, X. Liang, Y. Chen, *ACS Appl. Mater. Interfaces* 2016, *8*, 17728.
- **18** S. Burattini, H. M. Colquhoun, J. D. Fox, D. Friedmann, B. W. Greenland, P. J. F. Harris, W. Hayes, M. E. Mackay, S. J. Rowan, *Chem. Commun.* **2009**, 6717.
- 19 S. Burattini, B. W. Greenland, D. H. Merino, W. Weng, J. Seppala, H. M. Colquhoun, W. Hayes, M. E. Mackay, I. W. Hamley, S. J. Rowan, *J. Am. Chem. Soc.* 2010, *132*, 12051.

- **20** Y. Yanagisawa, Y. Nan, K. Okuro, T. Aida, *Science* **2018**, *359*, 72.
- 21 J. A. Neal, N. J. Oldenhuis, A. L. Novitsky, E. M. Samson, W. J. Thrift, R. Ragan, Z. Guan, *Angew. Chem. Int. Ed.* 2017, 56, 15575.
- 22 R. P. Sijbesma, F. H. Beijer, L. Brunsveld, B. J. B. Folmer, J. H. K. K. Hirschberg, R. F. M. Lange, J. K. L. Lowe, E. W. Meijer, *Science* 1997, *278*, 1601.
- 23 B. J. B. Folmer, R. P. Sijbesma, R. M. Versteegen, J. a. J. van der Rijt, E. W. Meijer, *Adv. Mater.* 2000, *12*, 874.
- 24 N. E. Botterhuis, D. J. M. van Beek, G. M. L. van Gemert, A. W. Bosman, R. P. Sijbesma, *J. Polym. Sci. Part A: Polym. Chem.* 2008, 46, 3877.
- **25** A. Gooch, C. Nedolisa, K. A. Houton, C. I. Lindsay, A. Saiani, A. J. Wilson, *Macromolecules* **2012**, *45*, 4723.
- **26** A. Feula, A. Pethybridge, I. Giannakopoulos, X. Tang, A. Chippindale, C. R. Siviour, C. P. Buckley, I. W. Hamley, W. Hayes, *Macromolecules* **2015**, *48*, 6132.
- 27 D. H. Merino, A. Feula, K. Melia, A. T. Slark, I. Giannakopoulos, C. R. Siviour, C. P. Buckley, B. W. Greenland, D. Liu, Y. Gan, P. J. Harris, A. M. Chippindale, I. W. Hamley, W. Hayes, *Polymer* 2016, 107, 368.
- **28** R. H. Zha, B. F. M. de Waal, M. Lutz, A. J. P. Teunissen, E. W. Meijer, *J. Am. Chem. Soc.* **2016**, *138*, 5693.
- 29 M. Hayashi, F. Tournilhac, Polym. Chem. 2017, 8, 461.
- **30** D. W. R. Balkenende, C. A. Monnier, G. L. Fiore, C. Weder, *Nat. Commun.* **2016**, *7*, 10995.
- **31** C.-C. Cheng, W.-T. Chuang, D.-J. Lee, Z. Xin, C.-W. Chiu, *Macromol. Rapid Commun.* **2017**, *38*, 1600702.
- 32 L. Montero de Espinosa, S. Balog, C. Weder, ACS Macro Lett. 2014, 3, 540.
- **33** D. W. R. Balkenende, R. A. Olson, S. Balog, C. Weder, L. Montero de Espinosa, *Macromolecules* **2016**, *49*, 7877.
- **34** S.-H. Tung, N. C. Kalarickal, J. W. Mays, T. Xu, *Macromolecules* **2008**, *41*, 6453.
- **35** B. J. Rancatore, C. E. Mauldin, J. M. J. Fréchet, T. Xu, *Macromolecules* **2012**, *45*, 8292.
- 36 P. Bai, M. I. Kim, T. Xu, Macromolecules 2013, 46, 5531.
- **37** P. Bai, J. Kao, J.-H. Chen, W. Mickelson, A. Zettl, T. Xu, *Nanoscale* **2014**, *6*, 4503.
- **38** K. H. Lee, P. Bai, B. J. Rancatore, B. He, Y. Liu, T. Xu, *Macromolecules* **2016**, *49*, 2639.
- **39** C.-M. Chung, Y.-S. Roh, S.-Y. Cho, J.-G. Kim, *Chem. Mater.* **2004**, *16*, 3982.
- **40** M. Burnworth, L. Tang, J. R. Kumpfer, A. J. Duncan, F. L. Beyer, G. L. Fiore, S. J. Rowan, C. Weder, *Nature* **2011**, *472*, 334.
- **41** R. Dong, Y. Liu, Y. Zhou, D. Yan, X. Zhu, *Polym. Chem.* **2011**, *2*, 2771.
- **42** P. Froimowicz, H. Frey, K. Landfester, *Macromol. Rapid Commun.* **2011**, *32*, 468.
- 43 J. Ling, M. Z. Rong, M. Q. Zhang, Polymer 2012, 53, 2691.
- 44 J. Zhan, M. Zhang, M. Zhou, B. Liu, D. Chen, Y. Liu, Q. Chen, H. Qiu, S. Yin, *Macromol. Rapid Commun.* 2014, *35*, 1424.
- 45 S. Ji, W. Cao, Y. Yu, H. Xu, Adv. Mater. 2015, 27, 7740.
- **46** E. Borré, J.-F. Stumbé, S. Bellemin-Laponnaz, M. Mauro, *Angew. Chem. Int. Ed.* **2016**, *55*, 1313.
- **47** A. O. Razgoniaev, E. V. Butaeva, A. V. Iretskii, A. D. Ostrowski, *Inorg. Chem.* **2016**, *55*, 5430.
- **48** We are using the word chromophore to denote "the part (atom or group of atoms) of a molecular entity in which the electronic transition responsible for a given spectral band is

- approximately localized." According to the IUPAC Goldenbook dx.doi.org/10.1351/goldbook.C01076.
- **49** Z. Wang, Y. Yang, R. Burtovyy, I. Luzinov, M. W. Urban, *J. Mater. Chem. A* **2014**, *2*, 15527.
- 50 Y. Li, S. Chen, M. Wu, J. Sun, *ACS Appl. Mater. Interfaces* 2014, *6*, 16409.
- 51 M. Wu, Y. Li, N. An, J. Sun, Adv. Funct. Mater. 2016, 26, 6777.
- **52** L. Chen, L. Si, F. Wu, S. Y. Chan, P. Yu, B. Fei, *J. Mater. Chem. C* **2016**, *4*, 10018.
- **53** R. G. Parr, In *Horizons of Quantum Chemistry: Proceedings of the Third International Congress of Quantum Chemistry Held at Kyoto, Japan, October 29–November 3, 1979; K. Fukui, B. Pullman, Eds.; Springer Netherlands: Dordrecht, 1980; pp 5–15.*

- 54 C. Lee, W. Yang, R. G. Parr, Phys. Rev. B 1988, 37, 785.
- 55 A. D. Becke, J. Chem. Phys. 1993, 98, 5648.
- **56** F.-S. Yen, L.-L. Lin, J.-L. Hong, *Macromolecules* **1999**, *32*, 3068.
- 57 E. Yilgör, E. Burgaz, E. Yurtsever, İ. Yilgör, *Polymer* 2000, 41, 849.
- 58 J. Mattia, P. Painter, Macromolecules 2007, 40, 1546.
- **59** G. A. Loughran, G. F. L. Ehlers, W. J. Crawford, J. L. Burkett, J. D. Ray, *Appl. Spectrosc.* **1964**, *18*, 129.
- **60** A. Plante, D. Mauran, S. P. Carvalho, J. Y. S. D. Pagé, C. Pellerin, O. Lebel, *J. Phys. Chem. B* **2009**, *113*, 14884.
- 61 A. Laventure, G. D. Grandpré, A. Soldera, O. Lebel, C. Pellerin, *Phys. Chem. Chem. Phys.* 2016, 18, 1681.

